

# A TRANSVERSE DEFLECTING CAVITY PROTOTYPE FOR THE MAX IV LINAC

D. Olsson\*, A. Bjermo, L. Christiansson, J. Lundh, D. Lundström, E. Mansten, M. Nilsson, E. Paju, L. Roslund, K. Åhnberg, MAX IV Laboratory, Lund, Sweden

## Abstract

The MAX IV LINAC operates both as a full-energy injector for two electron storage rings, and as a driver for a Short Pulse Facility (SPF). There are also plans to build a Soft X-ray Laser (SXL) beamline at the end of the existing LINAC. For SPF and SXL operation, it is important to characterize beam parameters such as bunch profile, slice energy spread and slice emittance. For these measurements, two 3 m long transverse deflecting RF structures are being developed. The structures are operating at S-band, and it is possible to adjust the polarization of the deflecting fields. In order to verify the RF concept, a short 9-cell prototype was constructed. The measurements results of the prototype are presented in this paper.

## INTRODUCTION

When the MAX IV LINAC [1] will be upgraded to a driver for an SXL [2], it becomes increasingly important to measure beam parameters such as bunch profile, slice energy spread and slice emittance. For these measurements, transverse deflecting structures are being designed. It is possible to change the polarization of the deflecting  $TM_{110}$  mode between horizontal and vertical by adjusting the phases of the RF signals that are fed to the structures. This is illustrated in Figure 1. Each structure is 3 m long, and consists of 91 cells, including 2 coupler cells. Two deflecting structures will be installed in the second half of 2019, and the RF concept is further presented in [3]. In order to verify the RF and mechanical concepts, a shorter prototype was constructed in early 2019.

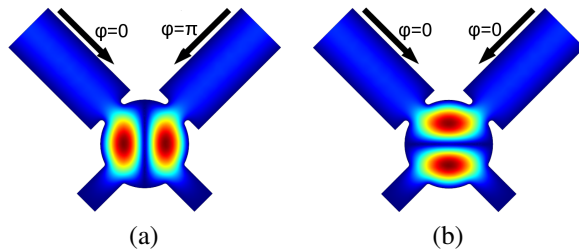


Figure 1: The magnitude of the electric field  $|E|$  in the coupler cell when deflecting the beam in the horizontal plane (a), and in the vertical plane (b).  $\varphi$  is the relative phase of the incoming RF signal.

## PROTOTYPE

The inner volume of the prototype is almost identical to those of the final structures. The only major difference is that the prototype has two coupler cells and 7 regular cells, while the final structures will have 2 coupler cells and 89 regular cells each. Figure 2 shows a CAD model of the prototype, and Figure 3 shows its inner volume.

The prototype was assembled using an in-house developed heat-shrink method. Here, each part is cooled in liquid nitrogen before it is mounted. The vacuum seal and RF contact to the rest of the assembly is then created when the part expands as it reaches room temperature. Unfortunately, some vacuum leaks were detected after all the parts were assembled. The copper was softened by heating the complete prototype in a bracing oven after it was assembled. This was necessary to create sufficient RF contact around the coupler cells. The heat-shrink assemble method will not be used when making the final structures. Instead, the coupler cells will be braced together, and the regular cells will be clamped together with a method similar to those presented in [4].

## MEASUREMENT SET-UP

The prototype and the test set-up can be seen in Figure 4. The fields are perturbed using a cylindrical bead attached to fishing line. The cylinder is moved along the structure by a stepper motor that is controlled from a MATLAB program via a Raspberry Pi. This set-up will also be used to characterize the final TDC structures, but longer rails are of course needed.

The mixed-mode S-parameters are measured with a 4-port network analyzer. As seen in Figure 1, the polarization is

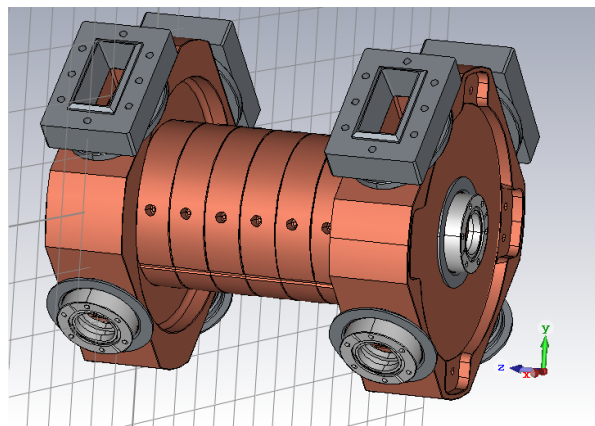


Figure 2: A CAD model of the 9-cell prototype.

\* Corresponding author: david.olsson@maxiv.lu.se

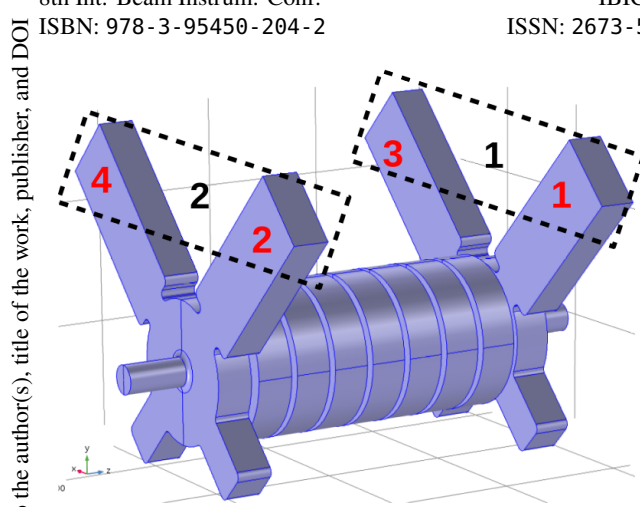


Figure 3: The vacuum body of the 9-cell prototype. The physical (red) and the logical ports (black) that are used during the mixed-mode measurements can also be seen.

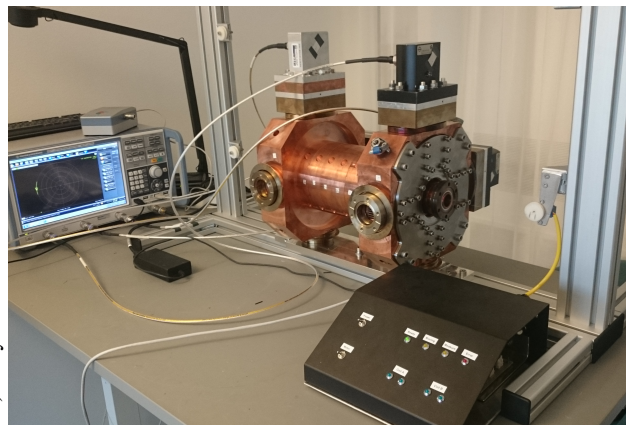


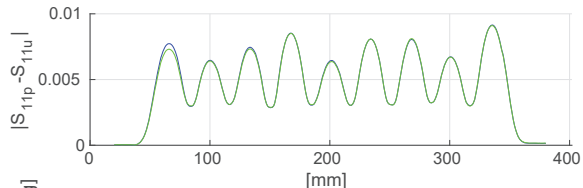
Figure 4: The prototype on the bead-pull test-stand during the measurements.

horizontal and vertical when feeding the input waveguides in differential and common-mode, respectively. During the measurements, the balanced logical port 1 consists of the physical ports 1 and 3, while the balanced logical port 2 consists of the physical ports 2 and 4. The port numbers are shown in Figure 3. The logical port indices are used when presenting S-parameter data in this report.

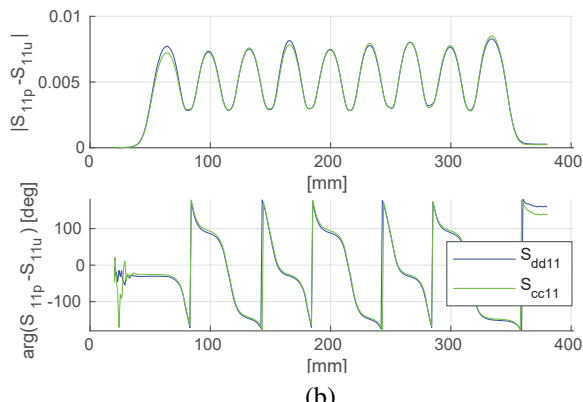
The same tuning procedure as described in [5] is being used. Tuning is done by deforming the cells using a dedicated tool. Since there is quite good isolation between the two excitation planes, it is possible to tune the horizontal and vertical planes independently of the other.

## RESULTS

Figure 5 shows the difference between the perturbed and unperturbed reflection parameter,  $S_{11p} - S_{11u}$ , along the structure at the corresponding vacuum operating frequency of  $f_c = 2.9985$  GHz before and after the tuning. Note that the magnetic and electric deflecting fields ( $\mathbf{B}_\perp$  and  $\mathbf{E}_\perp$ ) are



(a)



(b)

Figure 5: The difference between the perturbed and unperturbed reflection parameter,  $S_{11p} - S_{11u}$  along the structure at  $f_c$ .  $S_{dd11}$  and  $S_{cc11}$  are the reflection coefficient when exciting the structure in the horizontal and vertical plane, respectively. (a) and (b) are before and after tuning, respectively.

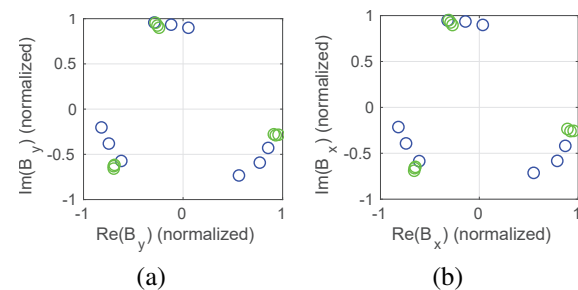


Figure 6: The measured deflecting field  $\mathbf{B}_\perp$  in the center of each cell, before (blue) and after (green) the tuning. In (a), the structure is excited in the horizontal plane, and it is excited in the vertical plane in (b).

proportional to  $\sqrt{|S_{11p} - S_{11u}|}$ . Also note that the nominal cell-to-cell phase advance is  $-2\pi/3$  (since it is backward-traveling structure), and that it is  $-4\pi/3$  for  $S_{11p} - S_{11u}$ .  $B_{x/y}$  in the origin of each of the 9 cells, before and after the tuning, are shown in Figure 6.

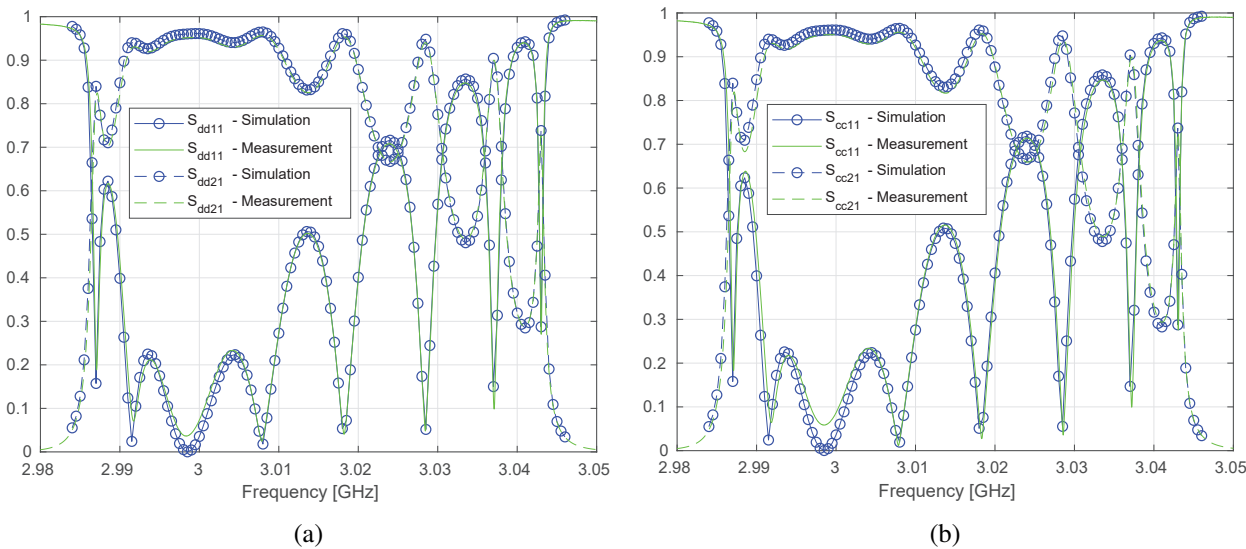


Figure 7: The simulated and measured reflection and transmission coefficients ( $S_{dd/cc11}$  and  $S_{dd/cc21}$ ) after the tuning. In (a), the structure is excited in the horizontal plane, and it is excited in the vertical plane in (b).

Figure 7 shows the simulated and measured reflection and transmission parameters of the full  $TM_{110}$  passbands after tuning. The simulations are performed in COMSOL Multiphysics, and there is good agreement to the measurements after the tuning. At  $f_c$ , we have  $S_{dd11} = -28.7$  dB, and  $S_{cc11} = -25.0$  dB.

## CONCLUSIONS AND FUTURE WORK

The work presented in this paper show that the RF concept that will be used in the MAX IV deflecting structures works, and it is possible to tune one polarization independently to the other. Measurements on the 9-cell prototype confirm this. Even though there are some vacuum leaks in the prototype, it might be possible to seal these leaks. If so, the prototype can, for example, be installed in the MAX IV gun test facility [6] and be used as a beam diagnostic tool. The two final 3 meter deflecting structures will not be assembled using the heat-shrink method. Instead, their pieces will be put together using traditional brazing and clamping. The final structures are being manufactured, and they will be installed in the MAX IV LINAC during a future shut-down. The plan is to have the complete RF deflecting system operational in 2020.

## ACKNOWLEDGEMENTS

Thanks to Louise Cowie at Daresbury Laboratory for lending us your coax-to-waveguide adapters.

## REFERENCES

- [1] S. Thorin *et al.*, "The MAX IV Linac", in *Proc. 27th Linear Accelerator Conf. (LINAC'14)*, Geneva, Switzerland, Aug.-Sep. 2014, paper TUOA03, pp. 400–403.
- [2] S. Werin *et al.*, "The Soft X-Ray Laser Project at MAX IV", in *Proc. 8th Int. Particle Accelerator Conf. (IPAC'17)*, Copenhagen, Denmark, May 2017, pp. 2760–2762. doi: 10.18429/JACoW-IPAC2017-WEPP025
- [3] D. Olsson, F. Curbis, E. Mansten, S. Thorin, and S. Werin, "Transverse RF Deflecting Structures for the MAX IV LINAC", in *Proc. 9th Int. Particle Accelerator Conf. (IPAC'18)*, Vancouver, Canada, Apr.-May 2018, pp. 3684–3687. doi:10.18429/JACoW-IPAC2018-THPAL027
- [4] D. Alesini *et al.*, "Design, realization, and high power test of high gradient, high repetition rate brazing-free S-band photogun", *Phys. Rev. Acc. and Beams*, vol. 21, 112001, 2018. doi:10.1103/physrevaccelbeams.21.112001
- [5] D. Alesini *et al.*, "Tuning procedure for traveling wave structures and its application to the C-Band cavities for SPARC photo injector energy upgrade", *Jour. of Inst.*, vol. 8, P10010, 2013. doi:10.1088/1748-0221/8/10/p10010
- [6] J. Andersson *et al.*, "The New MAX IV Gun Test Stand", in *Proc. 8th Int. Particle Accelerator Conf. (IPAC'17)*, Copenhagen, Denmark, May 2017, pp. 1537–1540. doi: 10.18429/JACoW-IPAC2017-TUPAB095